COVER PAGE

Bibliographical reference

Static Stiffness Method for Elastic Constants Determination of Anisotropic Acoustic Foams, Guqi Yan, Xinxin Guo, Bruno Brouard and Sohbi Sahraoui, Acta Acustica **vol. 103** (Number 4), 2017, pp. 650-656

DOI

https://doi.org/10.3813/AAA.919093

Acta Acustica united with Acustica
Vol. 103 (2017) 650 – 656

DOI 10.3813/AAA.919093

Static Stiffness Method for Elastic Constants Determination of Anisotropic Acoustic Foams

Guqi Yan, Xinxin Guo, Bruno Brouard, Sohbi Sahraoui
LAUM, UMR CNRS 6613, Université du Maine, Avenue Olivier Messiaen, 72085 Le Mans, France.
sohbi.sahraoui@univ-lemans.fr

Summary
This paper presents a method for the mechanical characterization of anisotropic foams. The objective of this study is to determine the static elastic parameters of an acoustic foam. The approach is based on measurements of the stiffness of samples in static compression and shear tests. The elastic constants are recovered through an inverse estimation method, by performing a fit of a numerical model (finite element method) with the measured stiffness of the porous material. The material is modeled as an orthotropic equivalent solid, whose principal directions are aligned with the coordinate system in which the experiments are conducted. A numerically generated target material is used here as a benchmark in order to show the efficiency of the approach. The method is applied to polyurethane (PU) foam, which is found to have orthotropic properties with highest stiffness in the direction parallel to the rise direction of the material.

PACS no. 43.20.e, 43.40.At, 43.40.Tm

1. Introduction

Acoustical porous materials (or sound absorbing materials) are commonly used in engineering applications to dissipate acoustical or mechanical energy (sound and vibration absorption or insulation, damping). During the last twenty years, many improvements have been made in both experimental and theoretical characterization of these materials. The modelling of porous materials is generally made at the macroscopic scale so that the heterogeneities can be averaged over a representative elementary volume.

Hence, the formalism of Continuum Mechanics is employed [1, 2]. Two classes of homogenized models are used to describe the dynamic behaviour of poroelastic materials: the equivalent fluid model, when the solid is assumed to be motionless, and the Biot theory formalism, when the frame is deformable. These homogenized models involve complex frequency dependent coefficients (densities, compressibility), whose expressions are given by empirical or semi-phenomenological models.

To characterize the viscoelastic properties of acoustic foams, some experimental techniques are available in the literature including non-resonant techniques [3, 4, 5], standing wave resonance of a longitudinally excited rod with end mass [6, 7], or mass-spring resonance [8]. All these methods are suited for measurements in a narrow frequency range. An extension of these measurement techniques for a wider frequency range has been made using theoretical modelling of foams viscoelastic behavior [9], through the frequency temperature superposition principle [10], or by means of acoustic excitations [11, 12]. A time domain method [13] may constitute an improved alternative to resonant and non-resonant techniques often used for dynamic characterization of polymers for the determination of viscoelastic moduli on a broad frequency range. It has been shown that the relaxation function obtained in a single static compression test was sufficient to calculate the complex modulus at any frequency.

Experimental tests are depending on the kind of materials. The mechanical tests such as tension or bending or technical measurements with strain gauges or ultrasonic propagation or Chladni method are usually chosen for hard materials. The mechanical characterization of soft materials such as PU foams are conducted in specific configuration such as loading in compression and shear with adapted instrumentation.

Due to the manufacturing process, porous materials, such as foamed polymers, exhibit highly anisotropic elastic properties. In the rising direction, non-regular cell geometry is induced which, in general, leads to highly directive cell orientations. Since Biot's contribution [14], numerous works were reported in the literature on the anisotropy of geo-materials [15, 16]. However, the acoustic materials studied after the Biot-Johnson-Allard theory [2] benefit especially from numerical investigations [17, 18]. More recently, Cuenca *et al* [19, 20] present static and dynamic methods for the inverse estimation of the nine elastic constants of orthotropic poroelastic foams. In these works, the authors use a cubic sample compressed along the three coordinate axes and give a numerical solution of the problem [21, 22]. The choice of the cubic geome-

Received 6 December 2016,
accepted 12 May 2017.

try was suggested by the anisotropic behavior of the material and the characterization. In the seismic mass method [19], the transfer functions were obtained through a laser vibrometer. In the static method [20], the field displacement of each face of the sample is measurement by means of 3D camera.

An alternative method consists on more simple experiments which don't need any optical and expensive apparatus used for isotropic foams [4] and for orthotropic foams [20]. This approach was recently used for characterization of isotropic foams [23] where the stiffness in compression is measured in two configurations: one brick-shaped sample having a square section and two juxtaposed identical samples. The present paper describes direct estimations of three Young moduli and three shear moduli in compression and shear tests respectively through the corresponding stiffness. The estimation error, evaluated by numerical simulation, is sufficiently small for long samples in compression test and thin samples in shear test. After this preliminary determination of six elastic moduli, an inverse estimation of the Poisson ratios is developed with three compression tests on cubic sample. Furthermore, the influence of the coupling with fluid phase is not considered in the study because it is insignificant at low crosshead speed or at low frequency [4, 5].

The main contribution of this paper is to propose a simple method for the static characterisation of the anisotropic, more specifically, orthotropic elastic properties of a porous material. As a proof of concept concerning the feasibility of the proposed inverse estimation approach, numerically simulated stiffness measurements are used as targets in the inverse estimation. The current paper starts with the material model and the characterisation method, which is then applied to a fictitious material, to verify the method and its practical application for PU foam characterization.

2. Elastic constants of foams

Commonly known open-cell foams exhibit a quasi-axisymmetric behaviour [22, 23, 24] and the rising direction during the foaming process, named longitudinal direction, is orthogonal to the transversely isotropic plane. However, for manufacturing reasons, the foam presents sometimes an orthotropic property with a largest Young's modulus in the rise direction.

As previously mentioned [23], the cubic geometry allows to test the isotropy or the degree of anisotropy by comparing the stiffness in the three directions. Foam plates usually provided by manufacturer are generally cut in the transverse plane defined here by T1 and T2 directions; the third rising direction is denoted L. During the industrial elaboration of plastic foams, these directions correspond to the extrusion direction (T1), the vertical rising direction (L) and their common perpendicular (T2). For the convenience, the coordinate system is denoted (x_1, x_2, x_3) corresponding to directions (T_1, T_2, L).

In fact, these foams are not homogeneous and their properties such as porosity, density and elastic constants depend on the measurement point. This discrepancy is observed for stiffness [23] and more recently for density [20] where the tested cubes present more than 15% deviation.

In order to characterize the mechanical properties of a porous material, it is necessary to establish a model for describing the elasticity of the porous frame without the influence of the fluid filling the pores. The equations lead to a Hooke's law for the frame, which can be written as

$$\sigma_i = C_{ij}\varepsilon_j, \tag{1}$$

where σ_i and ε_j contain the components of the stress and strain tensors according to

$$\boldsymbol{\sigma} = \left[\sigma_{11}, \sigma_{22}, \sigma_{33}, \sigma_{23}, \sigma_{31}, \sigma_{12}\right]^{\mathbf{T}} \tag{2}$$

and

$$\boldsymbol{\varepsilon} = \left[\varepsilon_{11}, \varepsilon_{22}, \varepsilon_{33}, \varepsilon_{23}, \varepsilon_{31}, \varepsilon_{12}\right]^{\mathbf{T}}, \tag{3}$$

and C_{ij} denotes the components of the stiffness matrix, which entirely characterizes the material.

The material under consideration is assumed to exhibit orthotropic symmetry, for which the compliance matrix, i.e., the inverse of the stiffness matrix, can be written as

$$S_{ij} = \begin{bmatrix} \frac{1}{E_1} & \frac{-\nu_{12}}{E_1} & \frac{-\nu_{13}}{E_1} & 0 & 0 & 0 \\ \frac{-\nu_{21}}{E_2} & \frac{1}{E_2} & \frac{-\nu_{23}}{E_2} & 0 & 0 & 0 \\ \frac{-\nu_{31}}{E_3} & \frac{-\nu_{32}}{E_3} & \frac{1}{E_3} & 0 & 0 & 0 \\ 0 & 0 & 0 & \frac{1}{2G_{23}} & 0 & 0 \\ 0 & 0 & 0 & 0 & \frac{1}{2G_{31}} & 0 \\ 0 & 0 & 0 & 0 & 0 & \frac{1}{2G_{12}} \end{bmatrix}, \tag{4}$$

where E_i is the Young's modulus along axis i, G_{ij} is the shear modulus in plane (i, j) and ν_{ij} is the Poisson's ratio for stress along i resulting in transverse strain along j. Furthermore, the symmetry of the compliance matrix leads to

$$\frac{\nu_{ij}}{E_i} = \frac{\nu_{ji}}{E_j}. \tag{5}$$

Then, if the principal material directions described above are given, the vector

$$\mathbf{x} = \left[E_1, E_2, E_3, G_{23}, G_{13}, G_{12}, \nu_{23}, \nu_{13}, \nu_{12}\right]^{\mathbf{T}} \tag{6}$$

contains the nine constants to be determined.

It is well known that the stiffness and compliance matrices must be positive-definite, a fact that may be used as constraints on the physical parameters in the estimation, as [25]

$$E_i > 0, \tag{7a}$$
$$G_{ij} > 0, \tag{7b}$$
$$1 - \nu_{ij}\nu_{ji} > 0, \tag{7c}$$
$$1 - 2\nu_{21}\nu_{13}\nu_{32} - \nu_{12}\nu_{21} - \nu_{13}\nu_{31} - \nu_{23}\nu_{32} > 0. \tag{7d}$$

Assuming that the principal material directions are known and aligned with the imposed coordinate, the stiffness method presented below allows to directly determine the Young and shear moduli with a reasonable error.

3. Stiffness method

Assuming that the principal material directions are known, the coordinate axes x_1, x_2, x_3 are chosen along these directions and the samples, extracted from a block of foam (Figure 1), are tested for determining their stiffness in compression and shear. The present method consists in measuring the three compression stiffnesses and the three shear stiffnesses to extract the approximate Young and shear moduli values. Other compression tests are performed on cubic samples in each direction. Hence nine tests on long ($S1$, $S2$, $S3$), thin ($S4$, $S5$) and cubic ($S6$) samples are performed for stiffness measurements and determination of whole elastic constants by inverse estimation. This summarized approach presented above is performed on an orthotropic fictitious material with an arbitrary set of parameters.

3.1. Compression and shear setups

In this section, compression and shear setups are presented. They are used for both numerical simulations and experimental measurements.

A simplified representation of the compression setup is given in Figure 2 where the material sample is placed between two rigid plates. Note that the displacement is solely applied on the top plate and that the bottom plate stays stationary during the experiment. Therefore the reference frame is the same for the compressed and uncompressed states and there is no rigid-body motion of the sample. In this test, the measured compression stiffness is F/u where the load F and the displacement u are defined in Figure 2

A simplified representation of the shear setup is given in Figure 3. The material samples are placed between a rigid plate and a U shaped profile. In shear test, we need two samples while only one sample is considered in numerical simulation. In this test, the measured shear stiffness F/u is twice the stiffness of each sample where F and u are defined in Figure 3.

The finite element model is based on software FreeFem++ by using P2 elements for the mesh. The boundary conditions are defined as follow: for compression test, the displacement in loading direction of the loaded face is equal to u, and zero in the two other directions, the opposite face is fixed (displacements equal to zero in three directions) and the other four faces are set to be free, as shown in Figure 2. As mentioned above, for shear test, the Figure 3 is simplified for numerical simulation where we need only one sample submitted to similar boundary conditions. The same program is used in these two configurations, only loading direction is modified to obtain shear or compression tests.

The samples $S1$, $S2$ and $S3$ (Figure 1) are used in the compression stiffness measurements in each direction. The side of the square section and the length of these parallelepiped samples are respectively a and L (Figure 2). The samples $S4$ and $S5$ concern the shear stiffness measurements. The side of the square section and the thickness of these parallelepiped samples are respectively b and h (Figure 3).

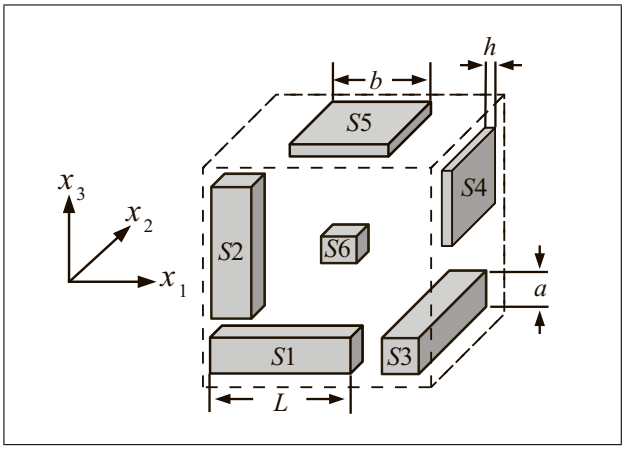

Figure 1. Samples orientation in a block of foam. Dimensions of samples: $S1$, $S2$, $S3$ (a^2L); $S4$, $S5$ (b^2h); $S6$ (a^3).

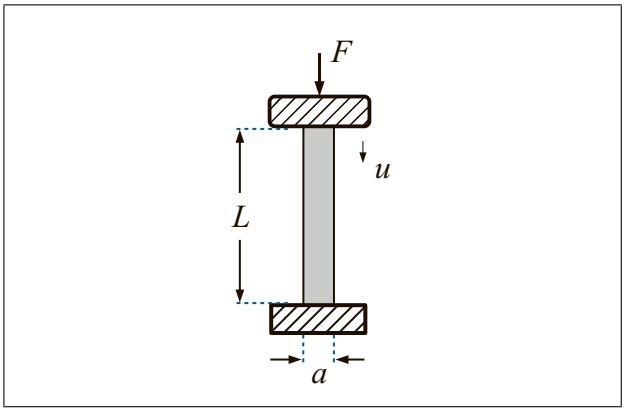

Figure 2. Compression configuration: sample (grey) between two rigid plates (cross-hatch).

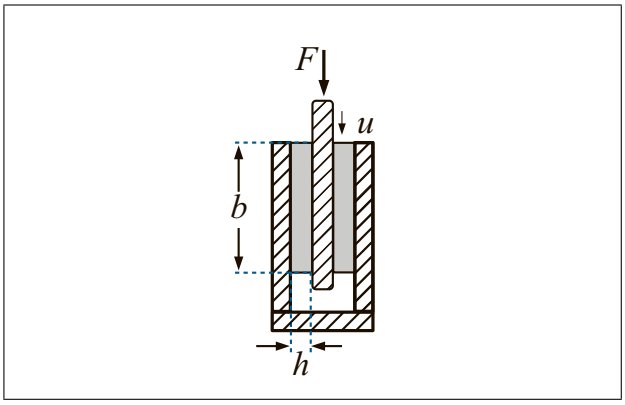

Figure 3. Shear configuration, samples (grey) squeezed between a rigid plate (cross-hatch) and a U shaped profile (cross-hatch).

For isotropic samples having a square section ($A = a^2$) and a length L, the compression stiffness can be written as [4]

$$K_c = \frac{EA}{L} f(\nu), \tag{8}$$

where E and ν are the Young modulus and Poisson ratio respectively and where the function f is depending on the

shape factor L/a. For high shape factor, the compression stiffness can be approximated by

$$K_c = \frac{EA}{L}, \tag{9}$$

and then E could be directly determined. To test this approximation in Equation (9), finite element compression simulations were performed at various shape factors L/a for a given isotropic foam (E = 185 kPa and G = 70 kPa). The approximate value of E is larger than the sought Young modulus and the error is decreasing for high shape factors (Figure 4).

By analogy with compression configuration (Equation (8) and (9)), shear tests (Figure 3) can be considered for the determination of the shear modulus G. The shear stiffness K_s of brick-shaped sample having a square section ($A = b^2$) and a thickness h (Figure 3) can be approximated by

$$K_s = \frac{2GA}{h} \tag{10}$$

for high value of the shape factor b/h. By finite element simulation, the error is evaluated for various shape factors b/h (Figure 4).

This numerical simulation of the influence of shape factors leads to expected results for sufficiently long and thin sample in compression and shear respectively. Nevertheless the high values of these factors, not convenient in compression tests, are limited in this study to 2 and 4 for compression and shear samples respectively.

The present approach is applied for anisotropic materials in the next sections where the approximate values of the Young moduli and the shear moduli are firstly determined through Equation (9) and (10).

3.2. Application to fictitious orthotropic material

To verify the presented stiffness approach, finite element simulations are performed on an artificial material, the parameters of the target material are chosen as E_1 = 210 kPa, E_2 = 330 kPa, E_3 = 420 kPa, G_{23} = 80 kPa, G_{13} = 110 kPa, G_{12} = 130 kPa, ν_{23}= 0.24, ν_{13}= 0.32, ν_{12}= 0.40. Following the notation in Equation (6), these chosen values, considered as a target for the inverse estimation procedure, are collected in vector $\mathbf{x_0}$.

The problem is solved in two steps described in the next subsections: the first step consists on the rough evaluation of the elastic constants through the measured stiffness K^{EXP} of each sample (Figure 1); in the second step, these approximate initial values, collected in $\mathbf{x_{ini}}$, are used for a more accurate inverse estimate.

3.2.1. Initial estimation of elastic moduli

In the first step, six tests are performed for the approximate evaluation of Young moduli and shear moduli based on the stiffness measurements. Then, for the estimation of the nine elastic constants including the Poisson ratios, three other tests are considered. The six samples $S1$-$S6$ (Figure 1) are used to obtain nine stiffness K_1-K_9. As detailed below, the nine tests are performed as follow: three compression tests with $S1$-$S2$-$S3$ samples and three shear tests with $S4$-$S5$ samples are conducted for the approximate evaluations of three Young's moduli and three shear moduli; three compression tests in each direction of S6 sample for the determination of three others stiffnesses.

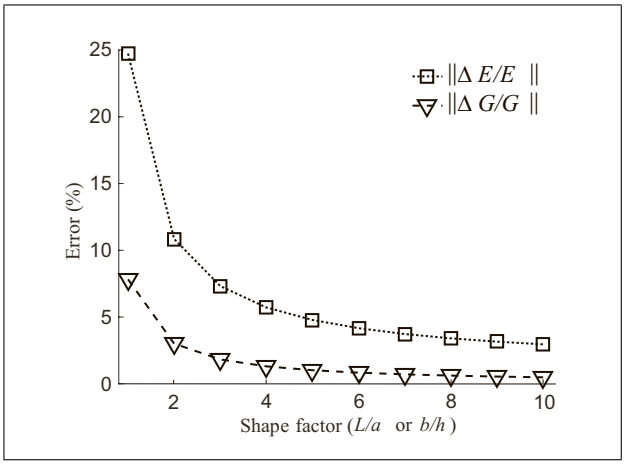

Figure 4. Influence of the shape factor on the approximate calculation of E and G for an isotropic material.

Table I. Target, initial and optimal elastic constants of fictitous orthotropic case.

$\mathbf{x}$	$\mathbf{x_0}$	$\mathbf{x_{ini}}$	$\mathbf{x_{opt}}$	$\|(\mathbf{x_0} - \mathbf{x_{opt}})/\mathbf{x_0}\|$
E_1 (kPa)	210	229.57	211.68	0.29 %
E_2 (kPa)	330	360.30	332.23	0.67 %
E_3 (kPa)	420	454.16	423.13	0.75 %
G_{23} (kPa)	80	79.31	80.11	0.13 %
G_{13} (kPa)	110	108.40	109.47	0.48 %
G_{12} (kPa)	130	127.58	130.14	0.10 %
ν_{23}	0.24	0.10	0.249	3.63 %
ν_{13}	0.32	0.10	0.311	2.88 %
ν_{12}	0.40	0.10	0.392	1.88 %

The finite element simulations are conducted in compression (Figure 2) on samples $S1$, $S2$ and $S3$ (Figure 1) having the same dimension ($40 \times 40 \times 80\,\mathrm{mm}^3$) in order to determine respectively the stiffness K_1^{EXP}, K_2^{EXP} and K_3^{EXP}. The approximate values of the Young moduli E_1 E_2 and E_3 extracted from the Equation (9) are collected in $\mathbf{x_{ini}}$ (Table I) and will be used in the inverse estimation. According to Figure 4, the approximate values of Young moduli are obtained with about 10% error. In the same way, the shear stiffness K_4^{EXP}, K_5^{EXP} and K_6^{EXP} corresponding to G_{23}, G_{13} and G_{12} are determined by means of shear tests (Figure 3) on the samples $S4$ and $S5$ (Figure 1) having the same dimensions ($80\times80\times20\,\mathrm{mm}^3$). The approximate values of these shear moduli obtained from Equation (10) are collected in $\mathbf{x_{ini}}$ (Table I) and will be introduced in the inversion procedure. It should be mentioned that the shear on $S4$ and $S5$ are sufficient for the three shear tests. In these numerical simulations, only one sample is used in the shear test. According to Figure 4,

the approximate values of shear moduli are obtained with about 1% error. Finally, three compression tests are realized on the cubic sample $S6$ ($40 \times 40 \times 40\,\mathrm{mm}^3$) along the directions x_1, x_2 and x_3 (Figure 1) for the determination of the stiffness K_7^{EXP}, K_8^{EXP} and K_9^{EXP}. The nine measured values K_1^{EXP}-K_9^{EXP} of the fictitious orthotropic material, obtained by finite element simulation, are used in the inverse estimation procedure presented in the next section.

3.2.2. Inverse estimation for optimal solution

In the inverse estimation procedure, a material model is varied to approximate the measured displacements. In each iteration of the optimization routine, a finite element model representing the experimental setup is solved for a proposed set of constitutive parameters. The recovery of the parameters is achieved by minimizing the quadratic relative differences between K^{FE} and K^{EXP} as shown in the following cost function:

$$f_0(\mathbf{x}) = \sum_{n=1}^{9} \left(\frac{K_n^{FE}(\mathbf{x}) - K_n^{EXP}(\mathbf{x_0})}{K_n^{EXP}(\mathbf{x_0})} \right)^2, \qquad (11)$$

where $\mathbf{x_0}$ contains the elastic constants of the fictitious material proposed above. The optimization procedure is implemented with a Matlab algorithm using Globally Convergent Method of Moving Asymptotes (GCMMA) [26]. The GCMMA routine consists in performing outer iterations and guarantees a strict decrease of the objective function (Equation (11)). For the details of these methods which are not the scope of this article, readers are referred to the articles of Svanberg [26, 27].

The six approximate values of Young and shear moduli obtained above and three arbitrary Poisson's ratios are the initial set of constitutive parameters noted $\mathbf{x_{ini}}$ (Table I) which are subjected to a number of numerical constraints, corresponding to the physical requirements of the material given by Equations (7). By repeating the optimization process using other starting points, the initial Poisson ratio don't influence the optimal solution; the value 0.1 is chosen arbitrarily.

4. Experiments

A polyurethane (PU) foam, kindly provided by Howa Tramico Company, is considered for the measurements of stiffness following the protocol described in Sec. 3. The compression and shear tests are performed by means of a standard tensile machine from Zwick/Roell (Z010) equipped with a 500 N load cell for the mechanical characterization of the sample at a fixed crosshead speed (10 mm/min) and at room temperature (20 °C).

4.1. Polyurethane foam samples

As mentioned above the principal directions are assumed known and correspond to the orientation of the foam samples (Figure 5) which are tested in compression (Figure 2) and in shear (Figure 3) following the same way used for

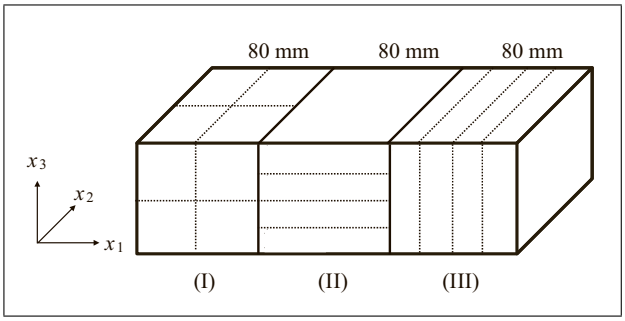

Figure 5. Orientation of polyurethane foam samples in the original batch (8 cubic samples in (I), 4 brick-shaped samples in (II) and (III)).

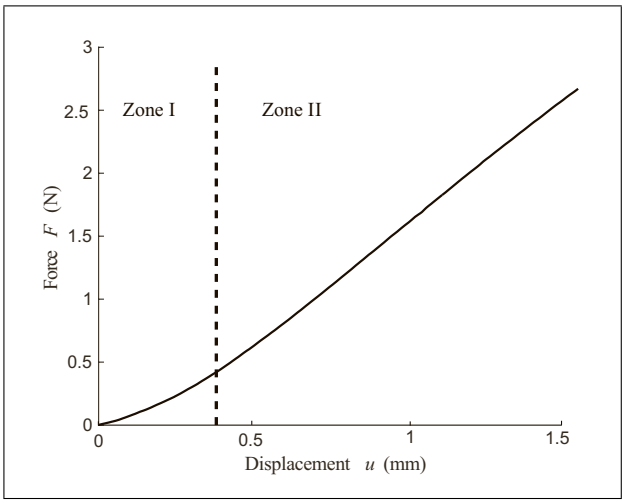

Figure 6. Static compression test for a cubic sample.

the numerical simulation for the fictitious material. To mitigate the impact of the heterogeneity on the measurement and for a better knowledge of spatial dispersion of the foam plate properties, a static compression stiffness evaluation has been performed on eight cubic samples; the resulting dispersion is about 9%. Thus the samples $S1$, $S2$ and $S3$ (Figure 1) are constituted of two juxtaposed cubic samples ($40^3\,\mathrm{mm}^3$) for compression tests. This juxtaposition technique previously used for characterization of isotropic foams [23] allows different compression tests with eight cubes. Two brick-shaped samples ($80 \times 80 \times 20\,\mathrm{mm}^3$) are needed for each shear test (Figure 1 and 5).

4.2. Compression and shear curves

The sample is compressed between two parallel plates covered with sand paper to avoid any slippage at the interface of the plates. For shear tests, sand papers and two samples (Figure 3) are also initially squeezed to avoid any slippage at the four interfaces.

In compression loading, the typical load-displacement curves (Figure 6) exhibit a first zone I where the slope ($\mathrm{d}F/\mathrm{d}u$) is increasing and a second zone II having a linear elastic behavior. The no-slip boundary conditions imposed by the rigid plates during the beginning of the loading cre-

ate interfaces with a complex strain distribution and shear stress where the collapse of the cells is followed by a static compression. In a deformation mapping study, Guastavino *et al*. [24] have observed a significant large gradient of the displacement near the loading plate which could confirm the interface zones mentioned above. For cubic samples (40 mm side), the width of the zone I is 0.36 mm (Figure 6) then the thickness for each interface can be estimated less than 0.18 mm. The first zone is governed by the interface process and presents an increasing of the slope. The second zone, corresponding to the compression state in the whole sample, is used for the stiffness determination. At higher strain until 10%, some studies [28] have indicated a decreasing slope zone corresponding to a bending regime and the beginning of beam cell buckling. It should be recommended that all the measured slopes correspond to the linear zone as well as in compression (Figure 6) or in shear (Figure 7).

In shear loading, the stiffness can be directly determinate from the load-displacement curve (Figure 7), but the strain compression fixed between 1% and 2% can affect the measured stiffness. This influence can be related to the imperfect cutting of shear samples and to the non-perfectly parallel faces. Accordingly, these aspects receive special attention in the exploitation of the load-displacement curves in compression (Figure 6) and in shear (Figure 7).

4.3. Results and discussion

Following the experimental protocol (Sec. 3) used for fictitious material, all the stiffness K_1^{EXP} -K_9^{EXP} in compression and shear tests are measured with the aim of determining the initial set of constitutive parameters $\mathbf{x_{ini}}$ and calculating the optimal solution $\mathbf{x_{opt}}$ (Table II). Despite the observed dispersion in the measured stiffness, an important assumption in the characterization procedure is that the foam block is homogeneous. Then, Young and shear moduli can be compared for each direction bearing in mind the sample stiffness deviation. In view of the foam heterogeneity, the first step devoted to the six moduli evaluation is relatively adequate with acceptable errors. However, these initial values are very useful in order to operate the optimization routine, for Poisson ratios determination. Assuming that the principal material directions are known and aligned with the imposed coordinate, the stiffness method presented above allows to directly determining the Young and shear moduli with a reasonable error (Table II).

The damping and dynamic elastic properties of solid materials, in acoustics and structural dynamics, are usually characterized through the concept of complex modulus of elasticity. These complex moduli can be obtained with classical approaches such as quasi-static measurement [4, 5] where the experiments are conducted through shaker excitation at various frequencies. In this way, the methodology presented in the present paper can be similarly used for the mechanical characterisation in the frequency domain. However, as mentioned in the introduction, a time domain approach [13] is able to predict the viscoelastic behaviour at any frequency. For this, the static

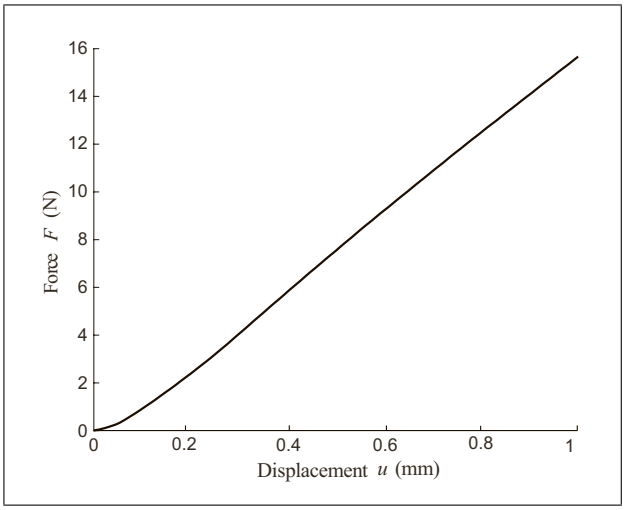

Figure 7. Static shear test for parallelepiped samples.

Table II. Initial and optimal orthotropic PU foam's elastic constants.

$\mathbf{x}$	$\mathbf{x_{ini}}$	$\mathbf{x_{opt}}$
E_1 (kPa)	201.38	200.37
E_2 (kPa)	335.48	331.13
E_3 (kPa)	411.42	389.96
G_{23} (kPa)	124.17	126.04
G_{13} (kPa)	111.86	113.76
G_{12} (kPa)	87.44	88.14
ν_{23}	0.10	0.485
ν_{13}	0.10	0.347
ν_{12}	0.10	-0.129

load-displacement curves (Figure 6, 7) used for the stiffness evaluation in compression and shear configurations can be completed by relaxation curves in each test. Then, for each test a linear load-time curve is followed by a decreasing load-time obtained at a fixed strain corresponding to the stress relaxation. The method is based on the adjustment of the stress-time relationship, obtained from relaxation tests on polymeric foams samples under static compression, with the four-parameter fractional-derivative Zener model. Thus, the frequency dependence of the viscoelastic moduli were calculated on a very broad range of frequency and compared to experimental value obtained by time temperature superposition method [10] from isotherm dynamic measurements on a narrow frequency and temperature domains. The results have shown a very good agreement between the experimental values and the prediction of the FZM. This approach is based on the adjustment of the stress-time relationship, obtained from relaxation tests on polymeric foams samples under static compression, with the four-parameter fractional-derivative Zener model.

5. Conclusion

In this paper a methodology for the inverse estimation of the elastic parameters governing the mechanical behaviour

of open-cell foams is presented. Nine static stiffness measurements of acoustic materials are performed to determine the elastic properties of orthotropic polyurethane foams. To verify the efficiency of the present approach, finite element simulations are performed on fictitious material. The application of the proposed method shows that a good agreement is reached between the optimal set of parameters and the targeted ones. The main originality lies in the simple measurements of stiffness for a straightforward extraction of approximate evaluation of Young's moduli and shear moduli. The more accurate elastic constants are estimated through an inverse estimation procedure. The developed approach, which requires load and displacement measurements during the characterization process, is a simple alternative. Furthermore this work highlights the spatial dispersion of foam plate's properties and the heterogeneity of these porous materials. Also, a special attention has been given to the boundary conditions as these may differ between the experiment and the numerical model, in particular, the bounding between the samples and the shear set up.

Acknowledgement

The authors would like to thank L. Guerry (Howa-Tramico) for foam supply.

References

[1] M. A. Biot: Theory of propagation of elastic waves in a fluid-saturated porous solid. i. low-frequency range. J. Acoust. Soc. Am. **28** (1956) 168–178.

[2] J.-F. Allard: Propagation of sound in porous media: modelling sound absorbing materials. Elsevier Applied Science, 1993.

[3] E. Mariez, S. Sahraoui, J.-F. Allard: Elastic constants of polyurethane foam's skeleton for Biot model. Internoise Congress Proceedings, Liverpool, 1996, 951–954.

[4] S. Sahraoui, E. Mariez, M. Etchessahar: Mechanical testing of polymeric foams at low frequency. Polym. Test. **20** (2001) 93–96.

[5] C. Langlois, R. Panneton, N. Atalla: Polynomial relations for quasi-static mechanical characterization of isotropic poroelastic materials. J. Acoust. Soc. Am. **110** (2001) 3032–3040.

[6] T. Pritz: Dynamic young's modulus and loss factor of plastic foams for impact sound isolation. J. Sound Vib. **178** (1994) 315–322.

[7] A. Sfaoui: On the viscoelasticity of the polyurethane foam. J. Acoust. Soc. Am. **97** (1995) 1046–1052.

[8] T. Pritz: Non-linearity of frame dynamic characteristics of mineral and glass wool materials. J. Sound Vib. **136** (1990) 263–274.

[9] T. Pritz: Analysis of four-parameter fractional derivative model of real solid materials. J. Sound Vib. **195** (1996) 103–115.

[10] M. Etchessahar, S. Sahraoui, L. Benyahia, J. F. Tassin: Frequency dependence of elastic properties of acoustic foams. J. Acoust. Soc. Am. **117** (2005) 1114–1121.

[11] J.-F. Allard, M. Henry, L. Boeckx, P. Leclaire, W. Lauriks: Acoustical measurement of the shear modulus for thin porous layers. J. Acoust. Soc. Am. **117** (2005) 1737–1743.

[12] V. Gareton, D. Lafarge, S. Sahraoui: The measurement of the shear modulus of a porous polymer layer with two microphones. Polym. Test. **28** (2009) 508–510.

[13] X. Guo, G. Yan, L. Benyahia, S. Sahraoui: Fitting stress relaxation experiments with fractional zener model to predict high frequency moduli of polymeric acoustic foams. Mech Time-Depend Mater **20** (2016) 523–533.

[14] M. A. Biot: Theory of elasticity and consolidation for a porous anisotropic solid. J. Appl. Phys. **26** (1955) 182–185.

[15] S. Crampin, Y. Gao: A review of a quarter century of international workshops on seismic anisotropy in the crust (0iwsa-12iwsa). J. Seismol. **13** (2008) 181–208.

[16] K. Helbig, L. Thomsen: 75-plus years of anisotropy in exploration and reservoir seismics: A historical review of concepts and methods. Geophysics **70** (2005) 9ND–23ND.

[17] N.-E. Hörlin, P. Göransson: Weak, anisotropic symmetric formulations of Biot's equations for vibro-acoustic modelling of porous elastic materials. Int. J. Numer. Meth. Engng. **84** (2010) 1519–1540.

[18] P. Göransson, N.-E. Hörlin: Vibro-acoustic modelling of anisotropic porous elastic materials: A preliminary study of the influence of anisotropy on the predicted performance in a multi-layer arrangement. Acta Acust. united Ac. **96** (2010) 258–265.

[19] J. Cuenca, C. Van der Kelen, P. Göransson: A general methodology for inverse estimation of the elastic and anelastic properties of anisotropic open-cell porous materials-with application to a melamine foam. J. Appl. Phys. **115** (2014) 084904.

[20] C. Van der Kelen, J. Cuenca, P. Göransson: A method for the inverse estimation of the static elastic compressional moduli of anisotropic poroelastic foams - with application to a melamine foam. Polym. Test. **43** (2015) 123–130.

[21] E. Mariez, S. Sahraoui: Measurement of mechanical anisotropic properties of acoustic foams for the Biot model. Internoise Congress Proceedings, Budapest, 1997, 1683–1686.

[22] M. Melon, E. Mariez, C. Ayrault, S. Sahraoui: Acoustical and mechanical characterization of anisotropic open-cell foams. J. Acoust. Soc. Am. **104** (1998) 2622–2627.

[23] S. Sahraoui, B. Brouard, L. Benyahia, D. Parmentier, A. Geslain: Normalized stiffness ratios for mechanical characterization of isotropic acoustic foams. J. Acoust. Soc. Am. **134** (2013) 4624.

[24] R. Guastavino, P. Göransson: A 3d displacement measurement methodology for anisotropic porous cellular foam materials. Polym. Test. **26** (2007) 711–719.

[25] R.-M. Jones: Mechanics of composite materials. Taylor and Francis, Philadelphia, PA, 1999, 519.

[26] K. Svanberg: A class of globally convergent optimization methods based on conservative convex separable approximations. Siam. J. Optimiz. **12** (2001) 555–573.

[27] K. Svanberg: The method of moving asymptotes - a new method for structural optimization. Int. J. Numer. Meth. Eng. **24** (1987) 359–373.

[28] A. Geslain, O. Dazel, J.-P. Groby, S. Sahraoui, W. Lauriks: Influence of static compression on mechanical parameters of acoustic foams. J. Acoust. Soc. Am. **130** (2011).